*J. Fluid Mech.* (1973), *vol.* 61, *part* 3, *pp.* 513–540
*Printed in Great Britain*



# A visual study of turbulent shear flow

By STAVROS G. NYCHAS†, HARRY C. HERSHEY AND ROBERT S. BRODKEY

Department of Chemical Engineering, The Ohio State University, Columbus

(Received 8 December 1972 and in revised form 19 June 1973)

The outer region of a turbulent boundary layer along a flat plate was photographed and analysed; in addition, limited observations of the wall area were also made. The technique involved suspending very small solid particles in water and photographing their motion with a high-speed camera moving with the flow.

The single most important event observed in the outer region was fluid motion which in the convected view of the travelling camera appeared as a transverse vortex. This was a large-scale motion transported downstream almost parallel to the wall with an average velocity slightly smaller than the local mean. It appeared to be the result of an instability interaction between accelerated and decelerated fluid, and it is believed to be closely associated with the wall-region ejections. The transverse vortex was part of a deterministic sequence of events; although these events occurred randomly in space and time. The first of these events was a decelerated flow exhibiting velocities considerably smaller than the local mean. It was immediately followed by an accelerated flow. Both these events extended from near the wall to the far outer region. Their interaction resulted in the formation of one or more transverse vortices. While the transverse vortex was transported downstream, small-scale fluid elements, originating in the wall area of the decelerated flow, were ejected outwards (ejection event). After travelling some distance outwards the ejected elements interacted with the oncoming accelerated fluid in the wall region and were subsequently swept downstream (sweep event). The sequence of events closed with two large-scale motions.

Estimated positive and negative contributions to the instantaneous Reynolds stress during the events were many times higher than the local mean values.

## 1. Introduction

The importance of the wall region, regarding not only momentum transport but other transport phenomena as well, has long been recognized. A realistic understanding of the processes inside this region would shed light on the nature of momentum transport and would permit the prediction of heat and mass transfer rates from measurements of only the turbulent field. To proceed from

† Present address: Max-Planck-Institut für Strömungsforschung, Göttingen, West Germany.

a background of phenomenological and statistical turbulence, one must obtain a better understanding of the mechanisms that are actually operating in the flow and upon which improved models can be built.

The literature for quantitative measurements very close to the wall has been reviewed by Corino & Brodkey (1969). Their direct visualization of the phenomena occurring in the wall region was an effort towards the understanding of the mechanisms of the flow in this region. Such research during the last fifteen years has given a fresh look at the whole subject. In what was considered to be a random phenomenon, a more or less coherent structure was uncovered. Moreover, a sequence of events in the wall area was observed. The events occur randomly in space and time but their sequence was found to be deterministic. A brief summary of these visual experimental findings will be given in this section. A detailed review of them can be found in Corino (1965), Corino & Brodkey (1969) and Kim, Kline & Reynolds (1971).

A combined dye-injection and hydrogen-bubble technique permitting quantitative measurements was developed by Kline and his co-workers (Runstadler, Kline & Reynolds 1963; Schraub & Kline 1965; Kline *et al.* 1967). They applied this method to an artificially tripped turbulent boundary layer. In the region $0 \leqslant y^+ \leqslant 10$ they observed a regularly distributed spanwise structure composed of low-speed streaks lifting up from the wall and moving downstream. These low-speed streaks are part of what Kline *et al.* (1967) called 'bursting', a sequence of events related to the production of turbulence. Kim *et al.* (1971) described bursting as being composed of three stages. The first was a lifting of a low-speed streak, creating an inflexional instantaneous velocity profile. This stage was followed by an oscillatory growth which after a few cycles was terminated by the onset of a more chaotic motion called 'breakup'. The process of 'bursting' was observed to be of an intermittent character.

Kim *et al.* observed that the most characteristic fluid motion during the oscillatory growth of the lifted low-speed streak was a streamwise vortex motion. Two other less common fluid motions were also observed during the second stage of 'bursting': (i) a transverse vortex (relatively rare) and (ii) a 'wavy motion' (more common). They reported that more than two-thirds of the cases studied involved a streamwise vortex. Increases in the scale of fluid motion by at least one order of magnitude were observed during the oscillatory growth. The scales were observed to be about $240y^+$ units, i.e. half the boundary-layer thickness.

Kim *et al.* excluded the possibility that the observed growth could have resulted from entrainment of the lifted low-speed streak by a large-scale motion. The arguments offered against such an entrainment process were the intermittent character and the fact that such an increase in the scale of fluid motions was the result only of an inflexional instantaneous velocity profile. According to the data of Kim *et al.* essentially all the turbulent energy production occurs during 'bursting' in the region $0 < y^+ < 100$.

Corino (1965) studied the wall area of a fully developed turbulent pipe flow. His technique was a visual method involving suspension of colloidal-size solid particles in a liquid as tracers. He photographed their motions with a high-speed motion-picture camera moving with the flow. He observed that the wall area

showed a distinct pattern characterized by a deterministic sequence of events occurring randomly in space and time. This pattern was a function of the distance from the wall. The area $0 \leqslant y^+ \leqslant 5$ (sublayer region) was found not to be laminar; it was characterized by velocity fluctuations of small magnitude and disturbed by fluid elements coming from the adjacent region. The area $0 \leqslant y^+ \leqslant 30$ was characterized by ejections of fluid elements away from the wall. These ejections were found to occur intermittently and randomly in both space and time; they were part of a sequence of events. The first event of this sequence was a *deceleration* of the axial velocity characterized by the essential disappearance of the velocity gradient and by a velocity defect as great as 50 % of the local mean velocity. The second event was an *acceleration*; i.e. a mass of fluid coming from upstream and entering at a $y^+$ of about 15 was directed towards the wall at angles of 0–15° and interacted with the fluid in the decelerated region. The third event was an *ejection*; i.e. an abrupt outward motion of fluid originating in the decelerated region. The fourth major event was the entry from upstream of a mass of fluid moving almost parallel to the wall, the *sweep* event. This latter higher speed fluid was often a part of the same mass of fluid as gave rise to the acceleration stage. The above cycle was repeated randomly in space and time.

Corino estimated roughly that 70 % of the $-\rho\overline{uv}$ Reynolds stress could be attributed to the ejections and 30 % (by difference) to the sweep events. More experimental findings, such as interactions between the events, frequency of occurrence and Reynolds number effects, can be found in Corino (1965). Wallace, Eckelmann & Brodkey (1972), by using hot-film anemometry techniques and by splitting the $uv$ signal into four parts, were able to measure approximately equal positive contributions to the Reynolds stress from ejections and sweeps, and negative contributions from their interactions (+ 70 % from ejections, + 70 % from sweeps and a total of − 40 % from the interaction of ejections and sweeps). Those values are for a $y^+$ of 15, the values being a weak function of position.†

Willmarth & Lu (1972), by using hot-wire anemometry and conditional sampling techniques, studied the structure of the Reynolds stress near the wall. They reported that 60 % of the positive contribution to the Reynolds stress $-\rho\overline{uv}$ occurred when the sublayer velocity was less than the local mean. Positive contributions to the instantaneous $uv$, 62 times higher than the local mean average, were measured. They concluded that the process of turbulent energy production in the wall region was intermittent and that 99 % of the contribution to $\overline{uv}$ occurred during 55 % of the total time.

Grass (1971), using the hydrogen-bubble technique developed by the Stanford group, studied visually and quantitatively the turbulent boundary layer in a free-surface channel flow. He mainly concentrated on surface roughness effects. Irrespective of wall roughness, he observed two well-defined flow events. These were

† It is important to distinguish between negative contributions to the instantaneous Reynolds stress and dissipation into heat. A negative $-\rho uv$ is a negative contribution (loss) to the turbulent energy production, when a time average of both positive and negative values is taken. High shear rates (created by high velocity gradients) give rise to large values of turbulent energy dissipation into heat (viscous).

ejections of low-momentum fluid outwards and 'inrushes' of high-momentum fluid towards the wall. His measurements indicated that the process of turbulent energy production is intermittent and that it occurs through the contributions of both ejections and inrushes. He concluded that the contribution of the inrushes to the turbulent energy production was mainly confined to the wall region. The role of the ejections, though, extended to the outer region, where very large positive contributions were measured.

Gupta, Laufer & Kaplan (1971), using a ten-hot-wire rake probe and by applying a conditional sampling technique, studied the spatial structure of the viscous sublayer. They used short averaging times and measured the correlation $R_{uu}$. Their data strongly suggested a coherent structure for the sublayer. Measurements of the instantaneous velocity in the spanwise direction uncovered a structure of local peaks and valleys reminiscent of the ones in laminar–turbulent boundary-layer transition. The mean spacing of the peaks was found to be equal to about 10 sublayer thicknesses.

Kovasznay, Kibens & Blackwelder (1970) developed and applied a conditional sampling technique. They measured time averages of the streamwise and normal mean velocities in a flat-plate turbulent boundary layer and extended their measurements to the streamwise fluctuating velocity component and spanwise vorticity component. They suggested that in the non-turbulent region the flow could be considered as an irrotational flow over a wavy displacement surface moving with a velocity equal to $0{\cdot}93U_0$ ($U_0$ being the free-stream velocity).

Blackwelder & Kovasznay (1972*a*, *b*) and Kovasznay *et al.* (1970) studied the large-scale motion in the intermittent region of a turbulent boundary layer. Conditionally averaged, space–time correlations were measured; their interpretation suggested the appearance of a random sequence of 'eruptions' or 'bursts' near the free stream.

Kaplan & Laufer (1969) used a conditional sampling technique to study the structure of the turbulent–non-turbulent interface and its relation to the entrainment process. Their measurements confirmed the results of Kovasznay *et al.* and complemented the observations concerning the behaviour of the 'bulges' of the interface. They found a small velocity defect between the trailing edge and leading edge of the 'bulges', the leading edge having a higher velocity. They concluded that the entrainment of non-turbulent fluid occurs mainly along the trailing edge.

Rao, Narasimha & Badri Narayanan (1971) concluded that the mean frequency of 'bursts' scales with the variables of the outer flow instead of the inner variables. Laufer & Badri Narayanan (1971) showed in addition that the convection time for an average wavelength of the turbulent–laminar interface (period of 'bulges') was of the same order as the average period $\bar{T}$ of the production cycle. The argument used to support this scaling with the variables of the outer flow is the fact that the non-dimensional period $U_0\bar{T}/\delta$ is independent of the Reynolds number $R_\theta$.

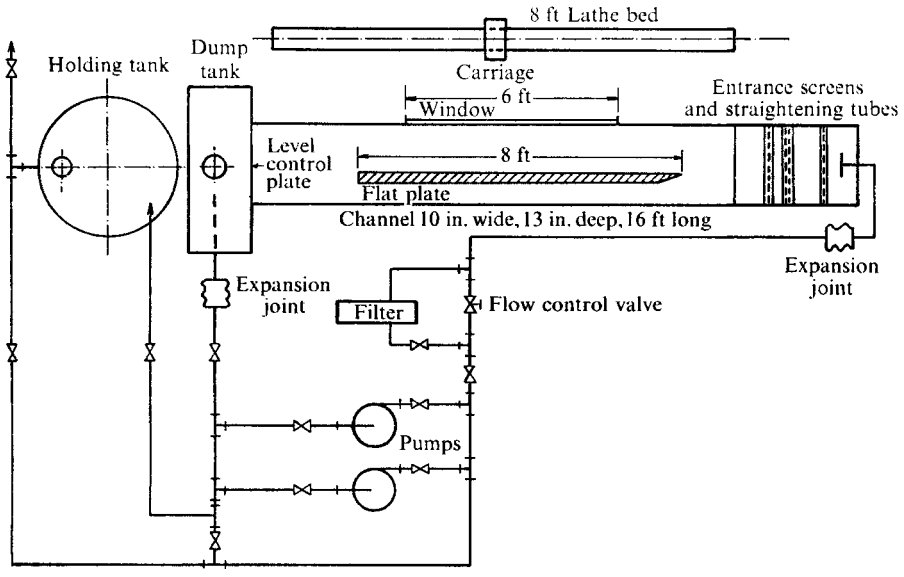


FIGURE 1. The visual flow system.

## 2. The experimental facility

The visual technique was designed to view the outer region, but it also permitted qualitative observations of those pertinent events of the wall region necessary to characterize this area. Specifically, a visual–photographic study of a flat-plate turbulent boundary layer was made. The technique involves suspending very small solid particles in water as tracers and requires no injection nor the introduction of any measuring device into the flow field. The motions of the particles were photographed by a high-speed motion-picture camera which moved with the flow. The dark-field illumination technique was the same as that used by Corino & Brodkey (1969) to study the wall area of a turbulent pipe flow. However, in contrast to their work, in the present effort the wall and the outer regions were both in view at the same time; the events and nature of the wall region could be easily identified. Most important, their relation to the outer region could be observed. Although the basic principle was essentially the same, considerable effort was devoted to the development to make the technique suitable for the present investigation.

Water was selected as the test fluid. The tracers were pliolite† particles having a diameter range of 44–74 $\mu$m. The density of pliolite is 1·026 g/cm$^3$ and its opitical properties with respect to light scattering are excellent.

The equipment was composed of three parts: the flow system, the flat plate and the photo-optical system. The flow system is depicted schematically in figure 1. The photo-optical system consisted of the light source, high-speed motion-picture camera and the camera carriage equipment. The ability to

† Commercial name of polyvinyltoluene butadiene, made by Goodyear Chemicals, Akron, Ohio.

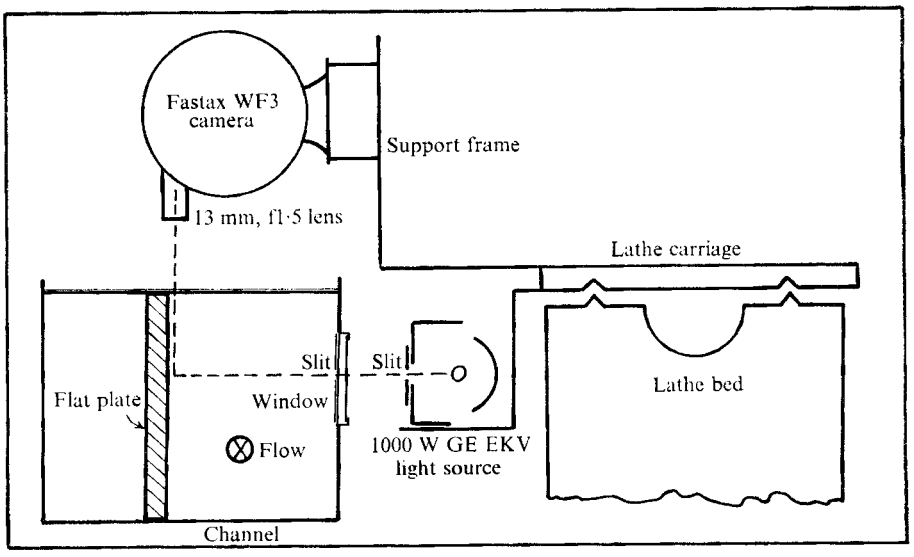


FIGURE 2. The photo-optical system.

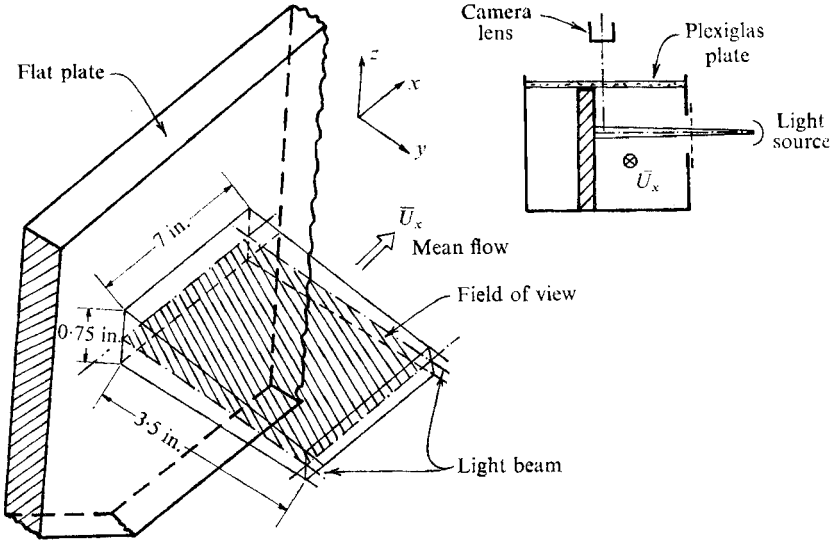


FIGURE 3. Camera viewpoint and field of view.

transport the camera and the light source at preselected velocities relative to the mean flow allowed the continuous observation of the development of a given flow phenomenon. Figure 2 is a schematic representation of the photo-optical system. The light beam passing through the glass window was scattered by the tracer particles and the scattered beam was photographed at an angle of 90°. Kodak no. 7278 Reversal Film was used at approximately 260 frames/s.

In figure 3, the camera viewpoint and the dimensions of the fields of view are given. The spanwise direction dimension corresponds to a $z^+ = zU^*/\nu$ of 150

to 200. This is the same order of magnitude as the expected spanwise variation; thus the view is essentially two-dimensional and gives little information about the $z$ direction.

In order to assure a fully developed turbulent flow, the boundary layer was tripped. The trip consisted of thin (1 mm approximate thickness) regular triangular elements placed side by side (Hama 1957).

For more details on the experimental system, one can refer to Nychas (1972), Corino & Brodkey (1969) and Brodkey, Hershey & Corino (1971). All of the problems and possible limitations raised in the latter two articles were reconsidered in the present work. Such details as the concentration of particles, particle shape, agglomeration of particles, modification of fluid viscosity and the adequacy of the particles to follow the flow accurately are discussed in Nychas (1972).

## 3. The sequence of events

In this section an overall view of the fluid motion events will be presented. In order to give the reader a coherent picture, sketches will be used to illustrate the various events. Only a few examples of actual measurements will be given. The bulk of these can be found in the thesis by Nychas (1972). In § 4, as a summary, a composite picture of the observations presented here will be given.

An overall examination of about twenty movies was conducted. Eleven of these were analysed in various degrees of detail. The analysis and establishment of the interconnexions of the flow events was a painstaking task owing to the complexity of the overall phenomenon. Everything described in this paper is much clearer in the motion pictures. Thus, a summary movie has been prepared and a selection of the most representative films analysed will be available for loan.†

The most important feature of both the wall ($0 = y^+ \sim 70$) and the outer region ($y^+ > 70$) of a turbulent boundary layer is the existence of a number of discrete events occurring in sequence, but randomly in space and time. The nature and scale of these events are different for the wall area and the outer flow; each is discussed in the following subsections.

The discussion is in terms of the non-dimensional distance $y^+$ rather than a distance normalized with the boundary-layer thickness. This was done for two reasons. First, the boundary-layer thickness could only be estimated and was not amenable to measurement as the fluid marker particles were both inside and outside the boundary layer. Second, the view of the camera moved along the flat plate and thus the boundary layer increased in thickness as the camera moved downstream. The layer properties were $\nu = 0{\cdot}0076\,\mathrm{cm^2/s}$, $U_\infty = 18\,\mathrm{cm/s}$, $U^* = 0{\cdot}80\,\mathrm{cm/s}$, $\delta = 4\,\mathrm{cm}$, $U^*\delta/\nu = 420$ and $R_\theta = 900$ for a typical run. The

† The summary movie will be available from the Motion Picture Division, Department of Photography, The Ohio State University, 156 W. 19th Ave, Columbus, Ohio 43210, U.S.A. Request *A Visual Study of Turbulent Shear Flow*. A service charge of $5.00 is made to cover replacement cost. The movie will also be available from the Engineering Societies Library, 345E. 47th St, New York 10017 U.S.A. The complete set of research movies can be seen by contacting Prof. R. S. Brodkey.

latter three values are an estimated average over the viewing range of the particular example. The variation in the computed $\delta$ was from 3 to 5 cm.

A drawback of the experimental technique used in this work is that it is difficult to distinguish between the rotational and the irrotational regions. If the vorticity were to be computed at many points, the interface between regions could be easily located. However, to evaluate the two derivatives required for the instantaneous vorticity at many points from the films would be a horrendous task, and hence was not attempted. In the future, however, a suggestion by Bradshaw (1973, private communication) that dye be injected at the front of the plate will be attempted. Perhaps by observing the dye plus the particles, the results of this work may be directly related to those of others who have studied intermittency and large eddy structures.

### 3.1. *Deceleration (low-speed fluid) event*

The first event observed was the appearance in the flow field of a decelerated region moving with a streamwise velocity lower than the mean. Most of the time the decelerated flow covered an area from the wall to a $y^+$ of about 500. Within this decelerated region the flow characteristics were regular; very chaotic motions or violent interaction were not observed. The event usually appeared in the field of view following a region where the flow moved with a velocity equal to or higher than the mean. The lower speed fluid gradually replaced the higher speed fluid. This decelerating effect was more pronounced in the outer region, where it appeared to move as a plug flow.

Although the present experimental technique did not allow reliable measurements of the velocity profile very close to the wall, it was visually observed that the plug-like character of the flow extended inside the wall region ($0 \leqslant y^+ \leqslant 70$). The disappearance of any appreciable velocity gradient throughout such a wide $y^+$ region was an important characteristic of the flow and was a striking thing to observe.

### 3.2. *Acceleration (high-speed fluid) event*

Following the low-speed fluid and while this event was still in view, a large-scale motion entered from upstream. Most of the time this fluid moved with a velocity higher than the local mean and first appeared in the field of view as a high-speed front covering a region of approximately $150 \leqslant y^+ \leqslant 400$. It should be emphasized that a real sharp distinct interface between the decelerated region and the entering higher speed fluid did not exist, although the line of demarcation was sharper as one approached the wall. In any event two regions could be distinguished, one of which moved downstream with a velocity higher than that in front of it. A sketch of these regions is presented in figure 4. This sketch, as well as subsequent sketches, are in the moving frame of reference.

As the high-speed fluid moves downstream it 'expands' both towards the wall and the outer region. The meaning of 'expands' can be best clarified by reference to figure 5. In this convected view, the accelerated fluid appears to displace gradually the decelerated fluid. This is shown by the change in the shape of the interface as it moves downstream. The field of view is covered more and more by

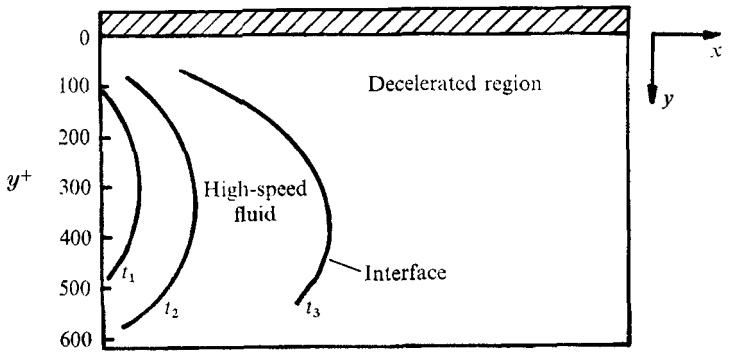


Co-ordinate convected at carriage velocity, $x$

FIGURE 4. Deceleration event and high-speed fluid (convected view). $t_1 < t_2 < t_3$.

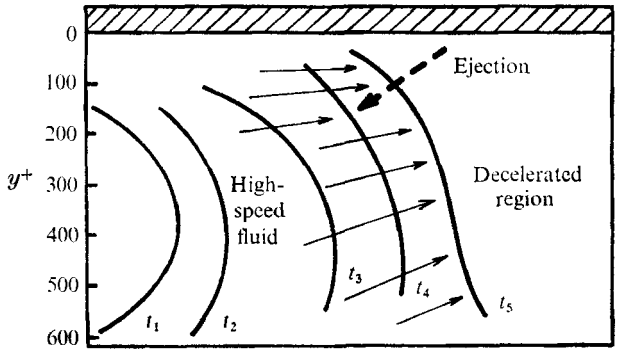


Co-ordinate convected at carriage velocity, $x$

FIGURE 5. Expanding high-speed fluid and ejection event (convected view).

the accelerated flow. It is in this context that the word 'expands' should be understood. A region of high shear is formed between the low-speed fluid adjacent to the solid wall and the higher speed fluid just next to it (in the positive-$y$ direction). The flow inside the high-speed fluid was directed at an angle towards the wall; this angle decreased and became almost zero for that part of the acceleration in the wall area.

The velocity of the high-speed fluid region was higher than the velocity of the decelerated region upstream of it. The average velocity profile during the time when the high-speed fluid event occurred was measured. There were cases where this conditional (pseudo-instantaneous) velocity profile was higher than the local mean and other cases where it was found to be lower than it. Figure 6 represents one case where the front speed is higher than the mean. The local mean velocities $\overline{U}_x(y^+)$ for the whole length of the motion picture and the logarithmic profile are given for comparison as well as the velocity of the deceleration region immediately preceding the high-speed fluid. The conditional time average for the acceleration event was about 1·5 s. At $y^+ = 100$, the local velocity of the high-speed fluid was about 26 % higher than the local mean. The plug-like character of the high-speed fluid region is clearly evident in figure 6. At $y^+ = 400$ the streamwise velocity of the accelerated region was about 55 % higher than that of the decelerated fluid.

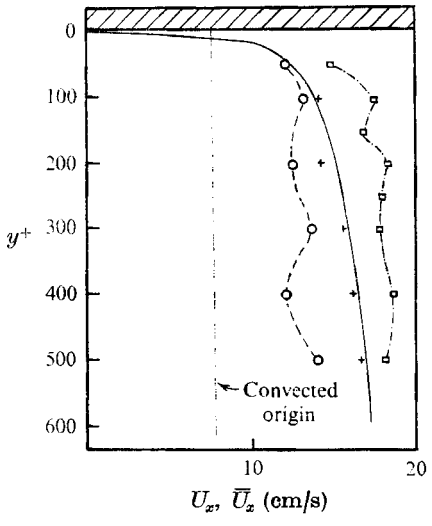


FIGURE 6. Velocity profiles for decelerated and accelerated regions and for the mean flow. □, $U_x$, high-speed fluid; +, $\bar{U}_x$, measured; ○, $U_x$, low-speed fluid; ——, $\bar{U}_x$, logarithmic profile.

| $y^+$ | 50 | 100 | 150 | 200 | 250 | 300 | 400 | 500 |
|---|---|---|---|---|---|---|---|---|
| $\bar{U}_x$ (cm/s) | 14·82 | 17·51 | 16·81 | 18·37 | 18·00 | 17·51 | 18·69 | 18·04 |

In the convected view of the travelling camera this difference in velocity is intensified and the acceleration velocity appeared 2·5 times higher than that for the deceleration. This was the reason why the entering accelerated fluid could be very clearly observed in the motion pictures.

### 3.3. *Ejection event*

The next event was a small-scale ejection that originated ($0 < y^+ \leqslant 50$) in the low-speed fluid region. As fluid was ejected outwards it more often violently interacted with the surrounding low-speed fluid although at times the interaction was absent. Eventually the fluid entered the high-speed fluid region. In some cases it was observed that ejected particles reached a $y^+$ of about 200 inside the high-speed fluid region. Most of the ejected particles observed reached a $y^+$ of 80–100 and then were swept downstream by the incoming high-speed fluid. The development of the high-speed fluid moving downstream and the ejection event are sketched in figure 5. Beyond a $y^+$ of about 100, the localized and violent nature of the flow events decreased, their character changed and their size increased.

In several instances during the time of ejection, fluid particles originating in the accelerated region moved at a slight angle towards the wall, passing very close to the ejected ones and not interacting with them. Apparently they were on different $x$, $y$ planes separated in the transverse $z$ direction (two-layer velocity effect). On fewer occasions, the ejected fluid element, after travelling a $y^+$ distance of about 30–40 units, turned back towards the wall, completed a loop and finally was swept downstream by the advancing high-speed fluid.

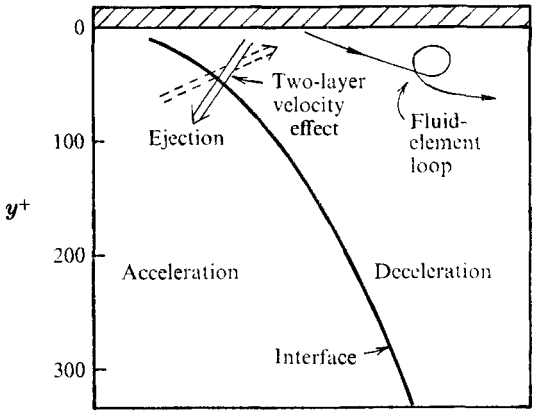


FIGURE 7. Two-layer velocity effect and fluid-element loop (convected view).

In figure 7 such a fluid-element loop and a two-layer velocity effect are illustrated. In table 1 some data on wall-area ejections are presented. More can be found in Nychas (1972). From the sign of the streamwise velocity fluctuations $u(t)$, it is clear that the ejections originated in a decelerated region. The largest outward angle $\phi_e$ observed was 31° and the smallest 2·0°. The ejection velocities $U_t$ were smaller than the local $\overline{U}_x$. An important point is that the magnitude of the normalized instantaneous Reynolds stress $(uv)/(U^*)^2$ is many times larger than the corresponding mean local value.

### 3.4. *Sweep event*

The part of the accelerated fluid in the wall region ($y^+ < 70$) is of particular importance. As was mentioned before, the demarcation line between high- and low-speed fluid close to the wall appeared sharper than for the outer flow. When a wall ejection occurred, it was the part of the accelerated region close to the wall which interacted with the ejected fluid particles and swept them downstream. The largest wallward angle $\phi_s$ observed for the sweeps was 10° and the smallest zero (flow parallel to the wall). Although the sweep event was an integral part of the accelerated region, it was its distinct role in the wall-area mechanism that distinguished it from the rest of the high-speed fluid. In table 2 some data on sweep events are given. Again, more can be found in Nychas (1972). It can be seen that, just as in the case of ejections, the magnitude of the instantaneous Reynolds stress is many times larger than the corresponding mean local value.

### 3.5. *Transverse vortices*

The single most important characteristic of the outer region was the existence of transverse vortices. In almost all cases, the transverse vortex was formed as follows. The interface of the advancing high-speed fluid front formed an angle with the wall as shown in figure 7. This resulted in a region composed of two large-scale streams of fluid moving almost parallel to each other and having

| Run | $y_{or}^+$ | $y_t^+$ | $\bar{y}^+$ | $U_x(t)$ (cm/s) | $\bar{U}_x(\bar{y}^+)$ (cm/s) | $u(t)$ (cm/s) | $v(t)$ (cm/s) | $-uv$ ((cm/s)$^2$) | $\frac{-uv}{U^{*2}}$ | $U_t$ (cm/s) | $\phi_e$ (deg) |
|---|---|---|---|---|---|---|---|---|---|---|---|
| M-132 | 38 | 66 | 52 | 9·70 | 12·25 | −2·55 | 3·60 | 9·17 | 14·25 | 10·30 | 20 |
| | 38 | 100 | 69 | 9·40 | 12·82 | −3·42 | 2·00 | 6·84 | 11·78 | 9·60 | 12 |
| | 70 | 100 | 85 | 10·00 | 13·35 | −3·35 | 1·45 | 4·86 | 7·55 | 10·15 | 8·2 |
| | 42 | 45 | 43 | 14·33 | 11·75 | 2·60 | 0·50 | −1·30 | −2·01 | 14·40 | 2·0 |
| M-133 | 28 | 46 | 37 | 1·60 | 11·00 | −9·40 | 0·80 | 7·52 | 11·80 | 1·65 | 26·0 |
| | 38 | 50 | 44 | 2·10 | 11·22 | −9·12 | 0·50 | 4·56 | 7·00 | 2·20 | 6·5 |
| | 50 | 94 | 72 | 5·80 | 11·81 | −6·01 | 1·60 | 9·62 | 15·05 | 6·00 | 15·5 |
| M-134 | 30 | 85 | 54 | 8·50 | 11·15 | −2·65 | 2·20 | 5·84 | 9·14 | 8·80 | 14·5 |
| | 40 | 65 | 53 | 10·90 | 11·15 | −1·25 | 2·60 | 3·25 | 5·08 | 11·20 | 13·0 |
| | 67 | 142 | 105 | 9·50 | 12·00 | −2·50 | 5·70 | 14·28 | 22·58 | 11·10 | 31·0 |

TABLE 1. Wall-area ejections. $y_{or}^+ = y^+$ of origin, $y_t^+ = y^+$ of termination, $\bar{y}^+ =$ average $y^+$, $U_t =$ actual velocity in this and subsequent tables

| $y^+_{or}$ | $y^+_t$ | $\bar{y}^+$ | $U_x(t)$ (cm/s) | $\bar{U}_x(\bar{y}^+)$ (cm/s) | $u(t)$ (cm/s) | $v(t)$ (cm/s) | $-uv$ ((cm/s)$^2$) | $\dfrac{-uv}{U^{*2}}$ | $U_t$ (cm/s) | $\phi_s$ (deg) |
|---|---|---|---|---|---|---|---|---|---|---|
| | | | | Wallward flow | | | | | | |
| 115 | 54 | 85 | 17·00 | 13·32 | 3·68 | −3·00 | 11·04 | 17·10 | 17·30 | 10·0 |
| 120 | 55 | 87 | 16·60 | 13·33 | 3·27 | −2·60 | 8·50 | 13·20 | 16·80 | 8·5 |
| 55 | 53 | 44 | 15·70 | 11·75 | 3·25 | −1·20 | 3·90 | 6·05 | 15·80 | 4·2 |
| 80 | 50 | 65 | 13·60 | 12·50 | 1·10 | −2·40 | 2·64 | 4·13 | 13·80 | 10·0 |
| 70 | 62 | 66 | 14·80 | 12·50 | 2·30 | −0·45 | 1·04 | 1·60 | 14·85 | 1·7 |
| 138 | 88 | 113 | 16·70 | 12·80 | 3·90 | −2·30 | 8·95 | 14·00 | 16·90 | 7·0 |
| 88 | 50 | 69 | 13·60 | 12·60 | 1·00 | −2·60 | 2·60 | 4·07 | 13·90 | 10·5 |
| | | | | Outward flow | | | | | | |
| 50 | 40 | 45 | 13·90 | 11·50 | 2·40 | −0·60 | 1·44 | 0·23 | 14·00 | 2·3 |
| 50 | 50 | 50 | 14·76 | 11·60 | 3·16 | 0·00 | 0·00 | 0·00 | 14·76 | 0 |
| 65 | 65 | 65 | 15·01 | 12·50 | 2·51 | 0·00 | 0·00 | 0·00 | 15·01 | 0 |
| 100 | 50 | 75 | 14·80 | 12·60 | 2·20 | −2·60 | 5·72 | 8·95 | 15·10 | 9·7 |

TABLE 2. Sweeps (runs M-132 and M-134)

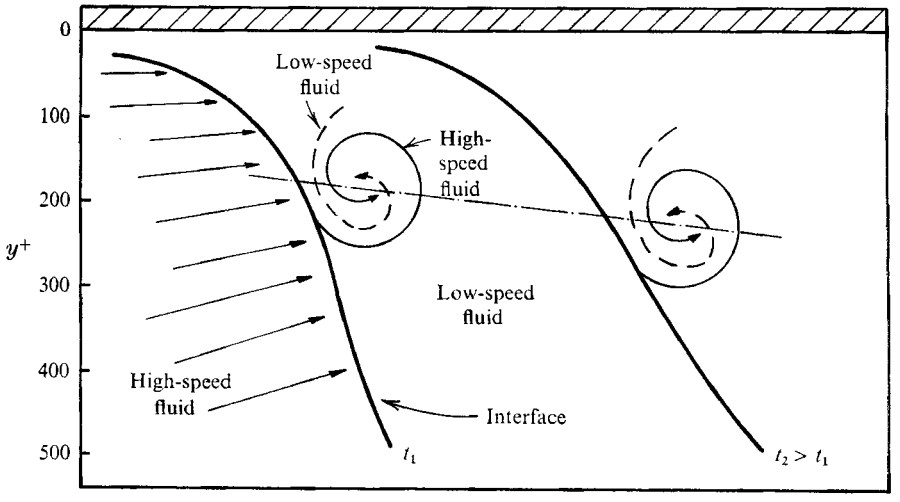


FIGURE 8. Forward transverse vortex, its relation to low- and high-speed fluid regions and its motion (convected view).

different velocities. Immediately after such a flow configuration had been established, a rotational large-scale motion developed. The transverse vortex appeared to be the result of a Helmholtz type of flow instability; the interface between the high- and low-speed fluid regions, being unstable, can give rise to such a vortex formation.

Figure 8 presents a sketch of a forward transverse vortex and its relation to the regions of high- and low-speed fluid. The vortex was transported downstream with a velocity slightly less than the local mean and at a slight angle with respect to the flat-plate wall. Most of the time during its downstream movement, the vortex moved away from the wall; there were some cases, though, where it moved towards the wall.

The transverse vortex was composed of both high- and low-speed fluid. Its scale changed slightly during its downstream movement; however an exact value could not be established, since a sharp interface between the rotating and non-rotating fluid did not exist. The approximate scale was equivalent to $200y^+$ units. The centre of rotation was located in a range of $y^+$ from about 200 to 400. In some films as many as five transverse vortices were observed while in others none were observed.

In a few cases where the angle of the entering high-speed fluid was relatively large, a reverse transverse vortex formed which rotated in the opposite direction to the forward transverse vortex. Usually the reverse vortex was followed by the formation of a forward one (figure 9). Their scales were of the same order.

In figure 10(*a*) one example of individual fluid particle paths and the downstream motion of a forward transverse vortex is presented. This particular vortex lasted for about 0·7 s and travelled a streamwise distance $x^+ = xU^*/\nu = 512$ before disappearing; its average velocity during that time was 11·9 cm/s compared with the local mean of 13·7 cm/s, i.e. about $0{\cdot}87\overline{U}_x$. It first appeared at

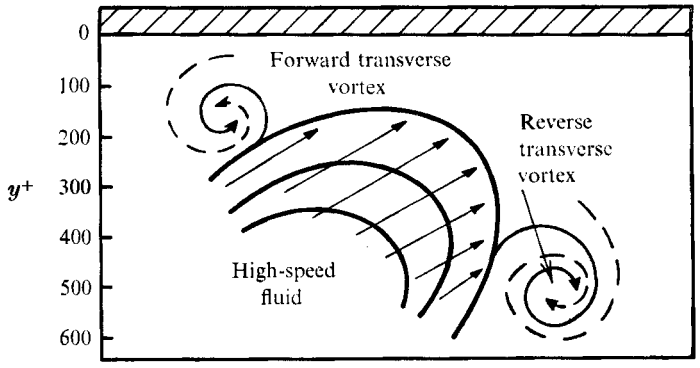


FIGURE 9. Reverse transverse vortex (convected view).

about $y^+ = 170$ and moved downstream parallel to the wall; its approximate diameter was $120y^+$ units. A modified convected view obtained by transposing the particle paths to make the vortex appear stationary at a point is presented in figure 10(*b*). In this figure the mechanism of Helmholtz instability is dramatically illustrated. Individual fluid particles ($G, H, K$) starting from a $y^+$ of about 400 move all the way to a $y^+$ of about 125 inside the vortex; one of them ($K$) is seen to loop around the stationary vortex centre and to be again directed downstream. Other fluid particles not participating in the vortex formation, but flowing around it, are shown; they give the picture of a flow past a cylinder with its axis in the spanwise $z$ direction. The participation of the low-speed fluid in the vortex formation is also shown here. One very important observation is the close association of the wall-area fluid ejections with the transverse vortices. Three wall ejections occurred at the same time as the vortex. Figure 11 (plate 1) is a streak photograph made in an effort to show the vortex (for the method, see Nychas 1972).

The following points should be stressed. First, it was the high-speed fluid region that was responsible for starting the vortex formation. In all the motion-picture runs, the transverse vortex always was associated with the high-speed fluid region. The low-speed fluid region appeared to be passive just before the onset of the transverse vortex. The only active region of the decelerated flow was the wall area where the ejections originated. The very small scale of the wall ejections and the extent of their penetration into the outer flow, for most of the cases, did not suggest that they caused the onset of the vortex motion. The accelerated fluid was the active agent for the onset of the Helmholtz instability and the subsequent creation of the transverse vortices.

The basic mechanism responsible for the formation of the reverse transverse vortex was the same as for the forward one. Figures 12(*a*) and (*b*) show an example of individual particle paths for this event. The modified convected view (stationary vortex) clearly shows the reverse-flow character of fluid particles belonging to high- and low-speed fluid. This can be seen by comparing this figure with that for the forward vortex (figure 10*b*). This particular reverse vortex lasted for

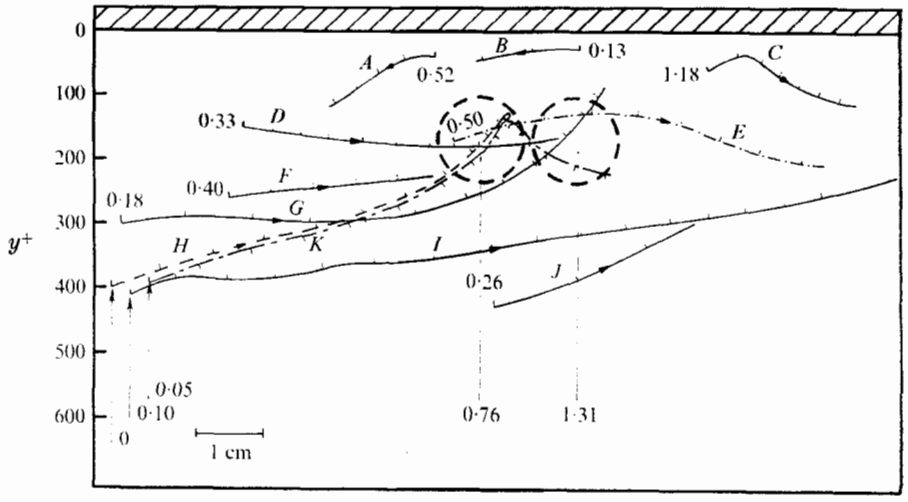


Co-ordinate convected at carriage velocity, $x$

(*a*)

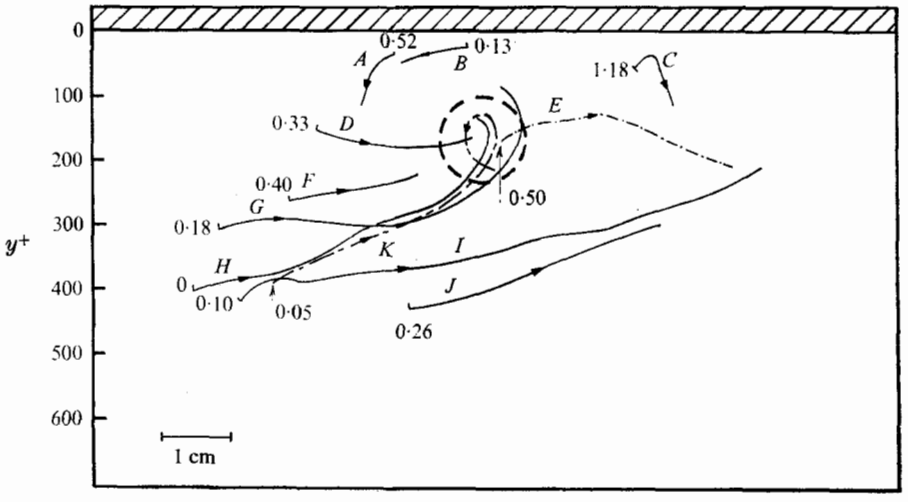


Co-ordinate convected at speed of vortex, $x$

(*b*)

FIGURE 10. Forward transverse vortex: individual particle paths. (*a*) Convected view. (*b*) Stationary vortex view. Letters mark particle paths and those on (*a*) correspond to those on (*b*). Numbers are time from zero in seconds.

0·68 s and its centre travelled a downstream distance $x^+ = 740$, moving parallel to the wall at $y^+ = 250$. Its average streamwise velocity was 13·3 cm/s compared with 15·6 cm/s for the local mean at $y^+ = 250$ ($\sim 0{\cdot}85\overline{U}_x$); its approximate diameter was $140y^+$ units.

In a number of cases two consecutive forward transverse vortices were formed along the same interface. The mechanism involved was the same, i.e., a Helmholtz

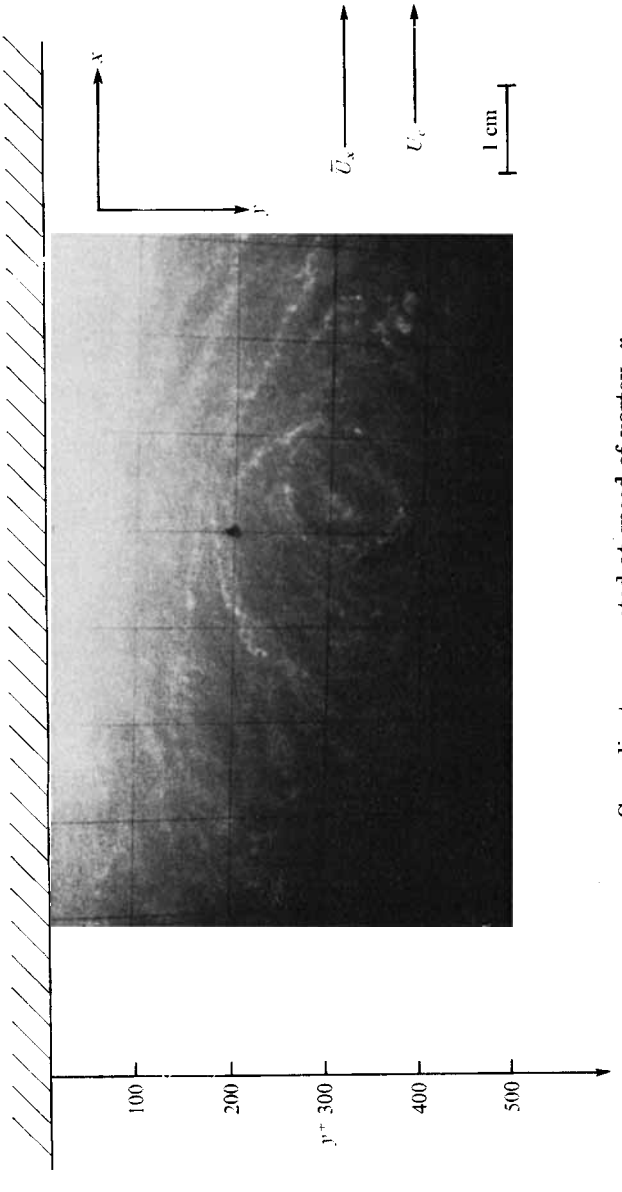


FIGURE 11. Streak photograph of forward transverse vortex.

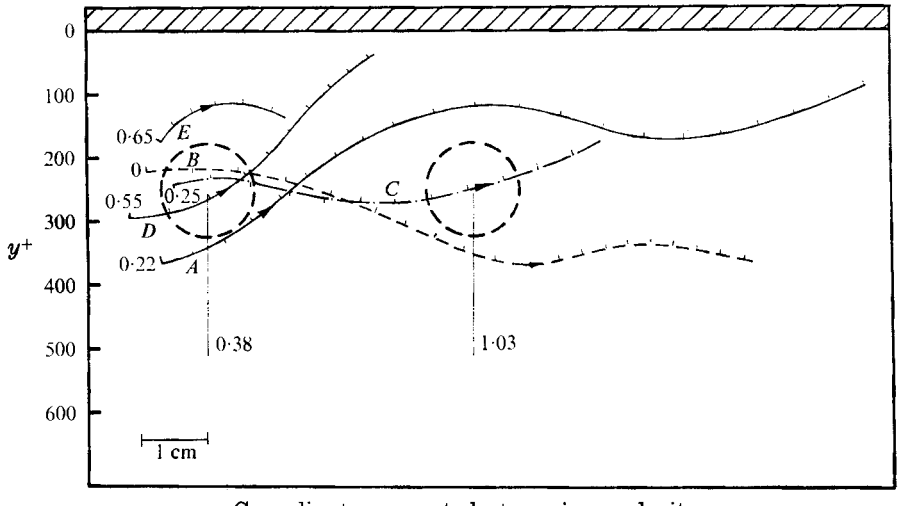


Co-ordinate convected at carriage velocity, $x$

(*a*)

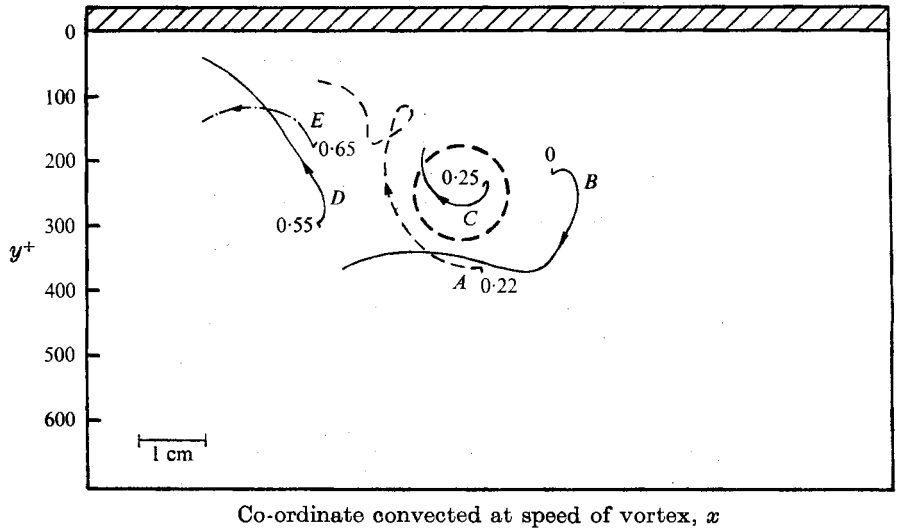


Co-ordinate convected at speed of vortex, $x$

(*b*)

FIGURE 12. Reverse transverse vortex: individual particle paths. (*a*) Convected view. (*b*) Stationary vortex view. Letters mark particle paths and those on (*a*) correspond to those on (*b*). Numbers are time from zero in seconds.

instability. After the first vortex had formed and travelled some distance downstream a second vortex appeared. There appears to be no difference in the nature and the characteristics of the second vortex, except that it was formed in a position closer to the wall than the first. In one movie as many as three consecutive vortices were observed; the third vortex was considerably smaller and lasted for a very short period of time in comparison with the first.

Estimated positive and negative contributions to the instantaneous Reynolds

| $y^+_{or}$ | $y^+_t$ | $\bar{y}^+$ | $U_x(t)$ (cm/s) | $\bar{U}_x(\bar{y}^+)$ (cm/s) | $u(t)$ (cm/s) | $v(t)$ (cm/s) | $-uv$ ((cm/s)$^2$) | $\frac{-uv}{U^{*2}}$ | $U_t$ (cm/s) | $\phi$ (deg) |
|---|---|---|---|---|---|---|---|---|---|---|
| | | | | | Wallward flow | | | | | |
| 212 | 200 | 206 | 18·70 | 14·70 | 4·00 | −1·90 | 7·60 | 11·80 | 18·80 | 6·5 |
| 200 | 232 | 216 | 18·10 | 14·72 | 3·38 | −2·60 | 8·80 | 13·66 | 18·30 | 9·5 |
| 296 | 264 | 280 | 22·80 | 15·73 | 7·07 | −4·60 | 32·50 | 50·40 | 23·20 | 11·5 |
| 396 | 320 | 358 | 19·80 | 16·35 | 3·45 | −2·75 | 9·48 | 14·70 | 20·00 | 12·7 |
| 480 | 460 | 470 | 19·10 | 16·72 | 2·38 | −0·65 | 1·58 | 2·45 | 19·20 | 2·5 |
| 460 | 434 | 447 | 19·90 | 16·70 | 2·20 | −2·00 | 4·40 | 6·82 | 20·00 | 5·8 |
| 508 | 492 | 500 | 19·20 | 16·73 | 2·47 | −0·65 | 1·59 | 2·46 | 19·30 | 2·5 |
| | | | | | Outward flow | | | | | |
| 112 | 136 | 124 | 15·50 | 13·98 | 1·52 | 2·40 | −3·65 | −5·65 | 15·70 | 9·0 |
| 180 | 200 | 190 | 15·50 | 14·65 | 0·85 | 2·00 | −1·70 | −2·64 | 15·70 | 7·5 |
| 234 | 316 | 300 | 17·90 | 16·01 | 1·89 | 0·80 | −1·51 | −2.34 | 18·00 | 2·5 |
| 320 | 344 | 332 | 14·70 | 16·18 | −1·48 | 3·20 | +4·74 | 7·35 | 14·90 | 15·5 |
| 400 | 434 | 417 | 19·50 | 16·60 | 2·90 | 2·50 | −8·40 | −13·02 | 20·10 | 7·3 |
| 470 | 430 | 450 | 22·30 | 16·70 | 6·60 | 2·60 | −17·20 | −26·70 | 22·40 | 6·7 |

TABLE 3. Study of a forward transverse vortex (run M-132)

| $y_{or}^+$ | $y_t^+$ | $\bar{y}^+$ | $U_x(t)$ (cm/s) | $\bar{U}_x(\bar{y}^+)$ (cm/s) | $u(t)$ (cm/s) | $v(t)$ (cm/s) | $-uv$ ((cm/s)$^2$) | $\frac{-uv}{U^{*2}}$ | $U_t$ (cm/s) | $\phi$ (deg) |
|---|---|---|---|---|---|---|---|---|---|---|
| | | | | | Wallward flow | | | | | |
| 296 | 284 | 290 | 14·20 | 15·74 | −1·54 | −1·30 | −2·00 | −3·15 | 14·30 | 11·0 |
| 284 | 258 | 271 | 12·60 | 15·73 | −3·13 | −2·60 | −7·87 | −12·23 | 12·90 | 11·7 |
| 188 | 126 | 157 | 10·50 | 14·60 | −4·10 | −3·85 | −15·80 | −20·55 | 11·00 | 19·2 |
| 70 | 36 | 53 | 10·30 | 12·25 | −1·95 | −2·50 | −4·38 | −6·77 | 10·60 | 13·5 |
| 176 | 134 | 155 | 11·30 | 14·59 | −3·29 | −3·90 | −12·82 | −19·80 | 12·00 | 19·0 |
| 270 | 216 | 243 | 14·00 | 15·50 | −1·50 | −1·10 | −1·65 | −2·56 | 14·10 | 4·5 |
| 366 | 356 | 361 | 10·50 | 15·70 | −5·20 | −0·95 | −4·94 | −7·67 | 10·50 | 5·0 |
| 172 | 134 | 153 | 14·60 | 14·59 | −0·01 | −2·70 | −0·02 | −0·03 | 14·90 | 10·5 |
| 258 | 210 | 234 | 13·00 | 15·35 | −2·35 | −1·60 | −2·76 | −4·27 | 13·20 | 7·0 |
| | | | | | Outward flow | | | | | |
| 116 | 138 | 122 | 11·20 | 13·98 | −2·78 | 1·00 | 2·78 | 4·28 | 11·30 | 4·7 |
| 216 | 246 | 131 | 14·70 | 14·08 | +0·62 | 1·65 | −1·02 | −1·58 | 14·90 | 6·5 |
| 260 | 316 | 288 | 15·60 | 15·74 | −0·14 | 3·20 | 0·45 | 0·70 | 15·90 | 11·5 |
| 316 | 366 | 341 | 12·00 | 16·20 | −4·20 | 1·90 | 7·98 | 12·39 | 12·10 | 8·5 |

TABLE 4. Study of a reverse transverse vortex (run M-132)

stress during the occurrence of the transverse vortices were many times larger than the local mean values. An example of each type is given in tables 3 and 4. More examples can be found in Nychas (1972).

### 3.6. *Large-scale inflows and outflows*

Another event observed was a large-scale inflow which usually dominated all of the outer region and sometimes even penetrated to the wall area. In the films, it appeared as a large region of fluid moving towards the wall with a small wallward angle. The streamwise velocity component of the event was close to the local mean. The motion was continuous from a $y^+$ of about 500 to about 100 and covered a streamwise area of about $x^+ = 1500$. Usually an inflow followed an outflow or vice versa or it occurred after a transverse vortex. It was easily distinguished from the acclerated or decelerated flow regions and was rarely observed to follow them. There were films where no large-scale inflows were observed and some where as many as two or occasionally three occurred.

The parts of the inflow which penetrated the wall area showed a similar character to the sweep events. Their wallward angles in the wall area were generally larger than the ones corresponding to the sweeps. Moreover, these wall inflows were rarely associated with wall-area ejections. The smallest wallward angle observed was 2·5° whereas the largest one was 17·5°. Very large positive or negative contributions to the instantaneous $-\rho uv$ Reynolds stresses were measured during the inflows.

The flow field during the large-scale inflow events appeared to be laminar-like and no violent interactions inside it were observed. Here again, no sharp demarcation line could be observed between the inflow region and the regions surrounding it. The inflow event appeared to be a stage during which the flow field re-established the mean velocity profile.

Large-scale outflows similar in scale to the inflow events were also observed They appeared as a region of fluid moving at a small angle away from the wall while being transported downstream with a velocity slightly lower than the local mean. Rarely, the fluid particles of an inflow after approaching a $y^+$ of 150 to 200 then started moving outwards, giving rise to a large-scale outflow. Most of the outflows observed originated from a region at $y^+ = 150$–$200$ and extended to $y^+ = 500$–$600$. In contrast to the inflows, which penetrated as far as the wall area, the outflows were observed to occur in the outer region only. The fact that they did not extend up to the wall area and that the outflowing fluid particles did not include elements originating from this region, distinguished them from the decelerated regions.

## 4. A composite picture

In the preceding section a somewhat detailed description of the nature of the turbulent motions in the outer and wall regions was presented. This, for the sake of clarity, was somewhat fragmented. In this section a summary of these observations in the form of a composite picture will be given.

In both the wall and outer regions distinct and identifiable events were observed. Each of these events was part of a deterministic sequence, although this sequence occured randomly in space and time.

The first of these events was a deceleration of the streamwise velocity extending from the wall to the outer region (figure 4). The degree of deceleration varied; deficiencies as great as 50 % of the local mean streamwise velocity were measured. While the flow field was decelerated, the second event, an acceleration of the streamwise velocity, occurred. It appeared as a large region of fluid entering from upstream and extending from the outer region to the wall area (figure 5). As the accelerated fluid moved downstream, it displaced and accelerated the decelerated fluid which was in front of it. This accelerating action occurred faster in the outer region than in the wall area. The change in the character of the fluid motion from the wall to the outer region was not abrupt. It occurred in a zone of approximately $70 < y^+ < 150$, which can be considered a sort of a transition area. Beyond a $y^+$ of about 150 the distinct character of the outer region manifested itself. The most important event in the outer region was a fluid motion which, in the convected view of the travelling camera, appeared as a transverse vortex (figure 8). This was a large-scale motion transported downstream almost parallel to the wall with an average velocity slightly smaller than the local mean. The formation of the transverse vortices appeared to be the result of an instability interaction (Helmholtz instability) between accelerated and decelerated fluid regions. One or more transverse vortices were formed by the interaction of the same accelerated and decelerated fluid regions. Although decelerated fluid participated in the formation of the transverse vortices, it was the accelerated fluid that was responsible for its participation. Both forward and reverse transverse vortices were observed (figure 9).

Very close to the wall the fluid motion was not laminar. Even in cases where fluid particle paths appeared rectilinear for some time, they were usually directed at some small angle. During a deceleration or acceleration event and before an ejection had occurred, the fluid motion appeared laminar-like for a short time. The most important events in the wall region were the ejections and sweeps (figure 7). These events occurred as follows: while the transverse vortex was transported downstream, small-scale fluid elements, originating in the wall area of the decelerated flow, were ejected outwards. After travelling some distance outwards, the ejected elements interacted with the oncoming accelerated fluid in the wall region and were subsequently swept downstream. These were energetic motions and their large positive contribution to the instantaneous Reynolds stress $-\rho uv$ has already been cited. The sweep events appeared equally energetic. The measurements of these also showed very large positive contributions to the instantaneous Reynolds stress.

Two large-scale fluid motions also were involved in the deterministic sequence of events. These were inflows and outflows; they both extended from the far outer region up to an area adjacent to the wall region. Usually an inflow followed an outflow or vice versa and occurred some time after the transverse vortex.

In the deterministic sequence of events, not all the events appeared all the time nor in exactly the same order; but for most of the cases they occurred as described.

## 5. Observations on a mechanism

An understanding of the mechanism of turbulent shear flow has been the aim of many recent papers already cited in the introduction. The sequence of events and the composite picture contribute to this and provide a coherent picture of what is occurring in the wall and outer regions of the flow and the interaction between these. From the implications of the visual study, one can make observations about and possibly elucidate upon the mechanism of turbulent shear flow. It is to this aim that this section is directed.

### 5.1. *The wall region* ($0 < y^+ < 70$)

The wall region appeared as the region where most of the turbulent energy was generated. The events responsible for the production of turbulent energy (as expressed by high positive values of the instantaneous Reynolds stress $-\rho uv$) were the ejections and sweeps. Furthermore, these events were very localized in space and time; thus, the processes of turbulent energy generation in the wall region would appear to be highly intermittent. This is also apparent from the data, where the positive contributions to the instantaneous Reynolds stress were as high as 40 times the local mean $-\rho\overline{uv}$. These observations are also supported by the work of Wallace *et al.* (1972), Willmarth & Lu (1972) and Gupta & Kaplan (1972) as cited in the introduction.

For a Newtonian fluid the rate of dissipation is equal to the square of the velocity gradient times the viscosity; i.e.

$$\tfrac{1}{2}\mu(\partial U_i/\partial x_j + \partial U_j/\partial x_i)^2.$$

Large gradients did exist at the interface between the accelerated and decelerated fluid. Since the interface was sharper in the wall area than in the outer region, the velocity gradients were higher along this interface than further out. When an ejection occurred, the ejected fluid elements penetrated into the accelerated region. Since the ejected fluid was actually low-speed fluid, the interface between it and the accelerated fluid also constituted a region of high velocity gradient. Thus the wall region is the area where most of the turbulent energy was generated and dissipated as heat. Some implications of this high gradient with regard to the energy balance have been made by Wallace *et al.* (1972).

The turbulent energy which was not locally dissipated was transferred by molecular means or convected towards the wall or the outer region. The molecular contribution was negligible outside of the sublayer. The deep penetration of the ejected wall fluid elements into the outer region is closely associated with such outward turbulent energy convection. The large values of $-\rho uv$ from the sweep events (i.e. that part of the acceleration within the wall region) can be associated with a wallward turbulent energy transfer. Whether this energy transfer extends to the viscous sublayer region is not evident from the present data and visual observations. The parallel to this from Corino & Brodkey (1969) has been discussed in the introduction.

The character of the sweep event depended on the local conditions in the wall

region. The sharper interface in this region prevented information from being transmitted from upstream. In this manner the action of the solid boundary (viscous effects) slowed down the propagation of upstream influences within the wall zone of the decelerated fluid. The fluid participating in the sweep event was part of the accelerated region and thus one understands why the sweep event also depends on the conditions of the outer flow.

The visual observations of this work did not indicate that the ejection events were directly dependent on wall-region conditions. The ejection event, with regard to its frequency of occurrence, was closely associated with the transverse vortices of the outer flow. This close association strongly suggests that the transverse vortices induce conditions in the wall region that cause an ejection to occur. The modification of the pressure field during the time of transverse vortex motion is an obvious candidate. Although there is still a great deal of doubt about the proper scaling parameters for the ejection frequency, visual observation supports the suggestion of Laufer & Badri Narayanan (1971) and Rao *et al.* (1971). It is also interesting to note that the low wavenumber convection velocity of wall pressure fluctuations ($\sim 0{\cdot}85U_\infty$; Wills 1970) is about the same as the mean velocity of the transverse vortices. The suggested connexion with the pressure field is obvious. Further, the small-scale induced ejections might be the cause of the high wavenumber pressure convection velocity ($\sim 0{\cdot}55U_\infty$). This velocity corresponds to the region where the ejections are observed. Yet it is known that the mean flow and probably also the high wavenumber part of the pressure fluctuations scale on inner variables.

### 5.2. *The outer region* ($y^+ > 70$)

The events in the outer region were deceleration, acceleration, transverse vortices, inflows and outflows. The cause of the creation of the deceleration and acceleration events was not apparent from the visual observations, but it can be said that the outer part of the regions depend on upstream flow conditions. The creation is no doubt related to the three-dimensional nature of the flow and its continuity implications. But no obvious causes of such velocity defects or excesses and for such a wide $y^+$ range were apparent.

As the high-speed fluid moved towards the wall region its character was more and more dependent on local conditions (i.e. the decelerated fluid in front of it). The decrease of wallward angles towards the wall region was a manifestation of this. Even after the interaction of low- and high-speed fluid in the wall region had progressed to some degree, the state of the outer part of the accelerated fluid depended mainly on the upstream history of the flow. This resulted from the convection of the history of flow events faster by the high velocities of the outer flow than the local influences could diffuse outwards from the wall region.

The high-speed fluid moved downstream faster than the decelerated region. At a given $x$ position the overlap between the high-speed fluid away from the wall and the decelerated region nearer the wall resulted in a highly inflexional instantaneous velocity profile. Such profiles have been reported by Kim *et al.* (1971). This is exactly the situation observed in free-stream shear layers (e.g. jets), the

only difference being that, in the outer region of the turbulent boundary layer, it is an unsteady developing situation. It occurred only when the acceleration event manifested itself. The visual observations suggested that the high-speed fluid caused the formation of the transverse vortices in the inflexional profile region and that the low-speed fluid participated in their formation but did not cause it. According to this picture, decelerated fluid moves outwards and accelerated fluid inwards during the vortex formation. This movement constitutes an entrainment of the low-speed fluid into the higher speed vortex region. The vortex travels some distance downstream owing to the continuously existing instantaneous inflexional velocity profile which feeds the Helmholtz instability.

The close association of the transverse vortices with the wall-region ejections must be emphasized. The high instantaneous rate of turbulent energy production, both positive and negative, during a transverse vortex motion could cause correspondingly high pressure fluctuations. Mollo-Christensen (1971) has commented on this. By a simple modification of the momentum equation, he arrived at a differential equation associating the pressure field with a turbulence production event. An analytic relation providing information about such pressure fluctuations is lacking. However, some qualitative remarks can be made. The wall zone of the decelerated fluid is at a higher pressure than that of the outer region at a given $x$ location during a transverse vortex motion. The justification for this can be obtained from a simple Bernoulli balance. If one adds to this already negative pressure gradient $dp/dy$ an instantaneous high pressure fluctuation, then an even larger pressure can occur in the wall region. This might be a mechanism that allows the transverse vortices to be one of the causes of the wall-region ejections. This proposition is further enhanced by the visual fact that the majority of the ejections were observed to be closely associated with the occurrence of transverse vortices. The present study does not exclude other possibilities creating favourable conditions for wall ejections to occur. It simply suggests one of them. Obviously, the whole question of the origin of wall ejections is still open and the suggestion made must be considered as conjecture.

The acceleration event is one of the mechanisms by which momentum from the outer flow is transferred towards the wall region. This is apparent from the large positive contributions of the acceleration event to the instantaneous Reynolds stress. The data also show that the accelerated fluid included some fluid elements moving away from the wall. This outward flow of high-speed fluid gives a negative contribution to the instantaneous Reynolds stress. The turbulent energy not locally dissipated is convected (or transferred by molecular means, which should be negligible here) towards and away from the wall. No conjecture can be made about what part of the non-dissipated turbulent energy is convected wallwards or outwards. It is further proposed that the transverse vortices are one of the mechanisms of exchange by convection between the outer and the wall regions. The other important events observed in the outer region are the large-scale inflows and outflows. Their role from a viewpoint of turbulent energy production, dissipation or exchange is not clear from the limited measurements. This is in spite of the fact that some instantaneous positive and negative contributions to $-\rho uv$ are many times higher than the local mean averages.

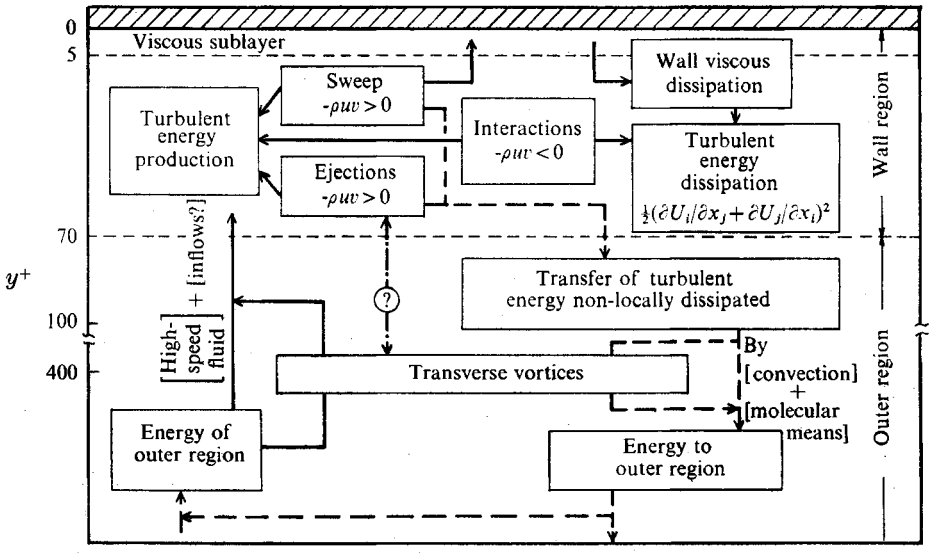


FIGURE 13. Turbulent energy production, dissipation and exchange.

In figure 13, a diagram of the turbulent energy generation, dissipation and exchange between the wall and outer regions based on the visual observations and measurements is presented. According to this diagram, turbulent energy is mainly generated in the wall region. The events responsible for this generation are the ejections, sweeps and their interactions; moreover the interactions of ejections and sweeps are responsible for high rates of viscous dissipation. The turbulent energy generated and not locally dissipated is partly transferred by molecular means and convected (by the sweeps) towards the sublayer region, thus contributing to this region's small velocity fluctuations and viscous dissipation at the wall. The rest of the non-dissipated energy is transferred outward mainly by convection. The balance of energy must be provided by the outer flow and the event mainly responsible for this transport is the accelerated flow. The transverse vortices act as an exchange mechanism for energy transfer from and to the wall region.

## 6. Implications and comparisons with the work of others

A major contribution to the literature on the mechanism of turbulent shear flow is the work of Kline *et al.* (1967) and Kim *et al.* (1971). However, in order to compare their work with ours, one should keep in mind some of the differences in the experimental techniques. Their camera was stationary and the filming speed was considerably slower. In the present work, the view of the travelling camera permitted the observations of developing flow events for longer times. This resulted in a more complete observation of a sequence of events *per se*. In spite of the different point of view and terminology used, general agreement between the two works can be recognized. In both cases, a deterministic sequence of flow events occurred randomly in space and time. In the wall region, the lifting

up of low-speed streaks corresponds to the ejections of the decelerated fluid in the present work. The region $10 \lesssim y^+ \lesssim 40$ where most of these streaks originated and their outward angles (from a maximum of 26° to zero) are in excellent agreement with the present observations.

A disagreement exists about the factors that give rise to an inflexion point in the velocity profile. In the present work a strongly inflexional velocity profile appeared in the shear region between decelerated and accelerated fluid. But it was the result of the gradual displacement of low-speed fluid by the much faster moving accelerated fluid. At the time of this displacement the decelerated fluid extended nearly throughout the whole boundary layer. According to Kim *et al.* the inflexional velocity profile was the result of a perturbation created by the lifting up of the low-speed streak.

Kline *et al.* and Kim *et al.* did not report any deceleration or acceleration events in the context of those reported here. This is apparently due to the limitations of their experimental technique. It may be recalled that the convected view of the camera greatly facilitated the observation of regions having velocity gradients by visually identifying their differences in velocity. Low-speed streaks as such were not observed in the present work; instead decelerated regions extending from the wall to the far outer region were found. This is due to differences in observations; the present experimental technique did not permit observations in the spanwise direction.

The transverse vortex of the present work was not the result of growth of smaller scale fluid motions; neither was its occurrence as rare as in Kim *et al.* More important, it was the outer accelerated fluid which caused its formation and not the 'triggering' action of the lifted low-speed streak. The higher frequency of occurrence of transverse vortices in the present work and the mechanism of their formation suggest, in contrast to Kim *et al.*, that they are one of the mechanisms of entrainment of higher speed fluid towards the inner zones.

Streamwise vortices as such were not observed in the present work. The failure to observe them might be due to limitations of the experimental technique, but this possibility seems unlikely. A streamwise vortex in the present observations should appear as a sequence of alternating inflows and outflows of comparable scale. Although in the present work usually inflows followed outflows and vice versa, they were of much larger scale. Moreover, they occurred as rather isolated fluid motions. Very rarely, small-scale fluid elements were observed to make one complete loop in the wall region; their scale did not grow any further. No definite conclusion can be drawn from the observation of these motions being part of streamwise vortices. The width of the light beam, which dictated the depth of field, was 0·75 in. at the flat-plate wall. This is equivalent to $z^+ = zU^*/\nu = 200$ in the transverse direction. At half the boundary-layer thickness the depth of field is equivalent to $z^+ = 167$. According to Kim *et al.* the scales of streamwise vortices grow up to half the boundary-layer thickness (i.e. $\frac{1}{2}\delta = 270y^+$). Such fluid motion could not be completely identified in the present work, even if the axis of these vortices coincided with the centre-plane of the light beam. Since the streamwise vortices of Kim *et al.* occurred randomly in the transverse direction, the probability of such a coincidence was very small.

There is an apparent similarity between the results of Kovasznay *et al.* and the present work. The outward movement of a 'lump' of fluid and its scale (our $y^+$ of 200 is equivalent to their $\frac{1}{2}\delta$) correspond in part to a forward transverse vortex. The sign of the angular momentum they suggested corresponds to the direction of rotation of a forward transverse vortex. In spite of this apparent similarity, there are differences in the two works which are based on the fact that in the present work only individual events were sought and no averages of any kind regarding the events were conducted.

A reinterpretation of the experimental results of Kovasznay *et al.* is possible in the light of individual events observed in the present work. It will be recalled that the occurrence of forward transverse vortices was more frequent than that of reverse ones. Moreover, for most of the cases the transverse vortices were transported downstream on a small outward angle. The low-speed fluid during the time of its participation in a forward transverse vortex moved away from the wall. Most of the wall-region ejections were closely associated with the transverse vortices. If one conducted a conditional sampling and averaging during these events, one would arrive at a picture of a 'lump' of fluid being ejected and rotating with an angular momentum compatible with the gradient $\partial\overline{U}_x/\partial y$. The combined effect of a transverse vortex and a large-scale outflow would intensify the picture of a lump of fluid moving outwards in such an averaging process; Kovasznay *et al.* suggested that the lump of fluid rotated because of the influence of an average velocity gradient characteristic of the local average conditions of its origin. In contrast, in the present work the forward transverse vortex had such a rotation because of the mechanism of Helmholtz instability involved in its formation. Kovasznay *et al.* failed to observe a reverse transverse vortex; this fact can be attributed to their averaging process. They did conclude that the flow in the 'fronts' (downstream) of the bulges is towards the wall, while in the 'backs' (upstream), the flow is directed outwards. This is in agreement with the present observations. The wallward flow in the 'fronts' corresponds to the wallward bending of the high-speed fluid during the formation of a forward transverse vortex.

With regard to the energy balance some comments are in order. First, the limited measurements of the present work do not form a statistical sample and hence they do not permit assigning a percentage contribution to $-\rho uv$ from the various events. Nevertheless, the qualitative conclusions drawn from these measurements are in agreement with the work of Wallace *et al.* (1972). The work of Grass (1971) is in excellent agreement with the present observations and measurements. Although he estimated that the inrushes (sweeps) should make the same positive contributions to the Reynolds stress as the ejections, he did not account for the negative contribution to this stress from their interactions. The work of Willmarth & Lu (1972) is in agreement with ours. They suggested that positive contributions to the Reynolds stress should be attributed not only to the ejections but also to the sweeps. In excellent agreement with the present data are their measurements of individual contributions to the instantaneous Reynolds stress, which were as large as 62 times the local mean. Kim *et al.* concluded that essentially all turbulent energy production in the area $0 \leqslant y^+ \leqslant 100$

occurred during bursting periods. The energy produced during non-bursting was either zero or very small. In the present work both ejections and sweeps contributed (positive contribution) to the instantaneous Reynolds stress. Their interactions contribute negatively to the instaneous $-\rho uv$.

National Science Foundation support, as well as support from The Ohio State University, made the present work possible. During the manuscript preparation, R. S. Brodkey held a NATO Senior Fellowship in Science at the Max-Planck-Institut för Strömungsforschung at Göttingen, West Germany. Their help is greatly appreciated.

## REFERENCES

BLACKWELDER, R. F. & KOVASZNAY, L. S. G. 1972*a* *Phys. Fluids*, **15**, 1545.

BLACKWELDER, R. F. & KOVASZNAY, L. S. G. 1972*b* *J. Fluid Mech.* **53**, 61.

BRODKEY, R. S., HERSHEY, H. C. & CORINO, E. R. 1971 An experimental facility for the visual study of turbulent flows. In *Turbulence Measurements in Liquids* (eds. G. K. Patterson & J. L. Zakin), p. 127. Department of Chemical Engineering Continuing Education Series, University of Missouri-Rolla.

CORINO, E. R. 1965 Ph.D. thesis, The Ohio State University.

CORINO, E. R. & BRODKEY, R. S. 1969 *J. Fluid Mech.* **37**, 1.

GRASS, A. J. 1971 *J. Fluid Mech.* **50**, 233.

GUPTA, A. K. & KAPLAN, R. E. 1972 *Phys. Fluids*, **15**, 981.

GUPTA, A. K., LAUFER, J. & KAPLAN, R. E. 1971 *J. Fluid Mech.* **50**, 493.

HAMA, F. R. 1957 *J. Aero. Sci.* **24**, 236.

KAPLAN, R. E. & LAUFER, J. 1969 *Proc. 12th Int. Cong. Appl. Mech., Stanford University*, p. 236. Springer.

KIM, H. T., KLINE, S. J. & REYNOLDS, W. C. 1971 *J. Fluid Mech.* **50**, 133.

KLEBANOFF, P. S. 1955 *N.A.C.A. Rep.* no. 1247.

KLINE, S. J., REYNOLDS, W. C., SCHRAUB, F. A. & RUNSTADLER, P. W. 1967 *J. Fluid Mech.* **30**, 741.

KOVASZNAY, L. S. G., KIBENS, V. & BLACKWELDER, R. F. 1970 *J. Fluid Mech.* **41**, 283.

LAUFER, J. & BADRI NARAYANAN, M. A. 1971 *Phys. Fluids*, **14**, 182.

MOLLO-CHRISTENSEN, E. 1971 *A.I.A.A. J.* **9**, 1217.

NYCHAS, S. G. 1972 Ph.D. thesis, The Ohio State University.

RAO, K. N., NARASIMHA, R. & BADRI NARAYANAN, M. A. 1971 *J. Fluid Mech.* **48**, 399.

RUNSTADLER, P. W., KLINE, S. J. & REYNOLDS, W. C. 1963 An experimental investigation of the flow structure of the turbulent boundary layer. *Dept. Mech. Engng, Stanford University Rep.* MD-8.

SCHRAUB, F. A. & KLINE, S. J. 1965 A study of the structure of the turbulent boundary layer with and without longitudinal pressure gradients. *Dept. Mech. Engng, Stanford University Rep.* MD-12.

WALLACE, J. M., ECKELMANN, H. & BRODKEY, R. S. 1972 *J. Fluid Mech.* **54**, 39.

WILLMARTH, W. W. & LU, S. S. 1972 *J. Fluid Mech.* **55**, 65.

WILLS, J. A. B. 1970 *J. Fluid Mech.* **45**, 65.